

## The metal-insulator transition and Fermi-liquid behaviour in the infinite-dimensional Hubbard model

This article has been downloaded from IOPscience. Please scroll down to see the full text article.

1994 J. Phys.: Condens. Matter 6 5439

(<http://iopscience.iop.org/0953-8984/6/28/018>)

View [the table of contents for this issue](#), or go to the [journal homepage](#) for more

Download details:

IP Address: 171.66.16.147

The article was downloaded on 12/05/2010 at 18:53

Please note that [terms and conditions apply](#).

# The metal–insulator transition and Fermi-liquid behaviour in the infinite-dimensional Hubbard model

S Wermbter and G Czycholl

Institut für Theoretische Physik, Universität Bremen, Postfach 330 440, D-28 334 Bremen, Germany

Received 10 March 1994

**Abstract.** We study the Hubbard model in dimension  $d = \infty$ , within an approximation that simultaneously reproduces the atomic limit and the weak-coupling limit up to second order in the interaction strength  $U$ . This method, which is a slightly modified version of an approximation suggested by Edwards and Hertz, is applied to the calculation of the self-energy and of the spectral function in the paramagnetic regime for different  $U$ , band fillings  $n$ , and temperatures  $T$ . We find Fermi-liquid behaviour for small  $U$  and (for half-filling  $n = 0.5$ ) a metal–insulator (Mott) transition at a critical value  $U_{cr}$ , but also a metallic non-Fermi-liquid phase for intermediate values  $U < U_{cr}$ . We compare our results with results obtained within the second-order perturbation theory in  $U$  and (at finite temperature) with the (essentially exact) quantum Monte Carlo (QMC) results. Qualitatively, the approximation reproduces the correct tendencies obtained by QMC, but in detail there are still discrepancies, in particular for intermediate values of  $U$ .

## 1. Introduction

Since the discovery of high-temperature superconductivity there has been a strong revival of theoretical interest in the Hubbard model (HM) [1, 2]. Though it has now been investigated for more than thirty years, a really satisfactory treatment and understanding of the model does not yet exist, with the exception of the one-dimensional case, where we know the exact solution for the ground state [3]. In dimensions  $d > 1$ , however, a reliable approximate solution, being applicable in the whole parameter regime (for example, in both the weak and strong coupling regime) is not available. A few years ago Metzner and Vollhardt [4] introduced the limit of infinite dimensions,  $d = \infty$ , for correlated lattice electron models like the HM. Meanwhile, it has been shown [5] that these models are greatly simplified for  $d = \infty$ , but that their essential properties are similar to those of realistic low dimensions  $d = 2, 3$ . Because of the simplifications one can hope to achieve, or at least come close to, the exact solution of the  $d = \infty$  HM, which would provide for a proper mean-field theory of the HM in a general dimension  $d$  [6, 7].

The simplifications in the limit  $d = \infty$  arise from the fact that the self-energy becomes site-diagonal. In other words, the local approximation of a momentum-independent self-energy  $\Sigma(z)$ , which has frequently been used before without justification, becomes exact in this limit [4–9]. This can be shown most easily using the standard (self-consistent Feynman diagram)  $U$ -perturbation expansion for the self-energy in terms of skeleton diagrams (containing only full Green function lines); here all types of diagrams exist as for finite  $d$ , but only those containing only the local (on-site) propagator survive the large- $d$  limit. Consequently, all theorems and rules based on the standard perturbation treatment, for example the Luttinger theorem [10] and the Kadanoff–Baym [11] scheme for constructing

conserving approximations, are applicable for  $d = \infty$  as for finite  $d$ . The HM remains, in particular, non-trivial for  $d = \infty$ , and a naive mean-field treatment like the Hartree approximation does *not* become correct. But the fact that only the local on-site propagator  $G(z)$  occurs in the skeleton diagram expansion of the self-energy  $\Sigma(z)$  means that the self-energy must be a functional of  $G(z)$  alone [12]:  $\Sigma(z) = S[G(z)]$ . Therefore, the self-energy knows about the lattice only via the local propagator. Because the same type of skeleton diagrams occurs this functional dependence  $S[G]$  must be the same as in the case of an atomic problem [6, 12] or of an impurity problem like the single-impurity Anderson model (SIAM) [13]. In other words, the functional dependence  $S[G]$  is universal for a large class of models. Unfortunately, one does not know the exact functional form of  $S[G]$ ; the trivial solution of the atomic problem yields the explicit form  $\Sigma_{\text{at}}(z)$  but not its functional dependence on the (atomic) propagator. Brandt and Mielsch [12] have shown that in principal one can obtain the functional dependence by solving the atomic problem in the presence of two time-dependent external fields acting on spin-up and spin-down electrons. But this problem (with *two* auxiliary Kadanoff–Baym [11] fields) is also not exactly solvable. However the  $d = \infty$  Falicov–Kimball model (FKM) [14], i.e. a simplified version of the HM for which only the electrons of one spin direction are mobile, could be solved exactly [12], because then only one auxiliary field is needed. For the general  $d = \infty$  HM (i.e. two auxiliary fields) only numerical (Monte Carlo) treatments have been possible up to now, using a time discretization of the auxiliary fields [15] or using the equivalent mapping to the Anderson impurity model [13]. As the SIAM can efficiently be treated by means of quantum Monte Carlo (QMC) methods, this mapping and the subsequent QMC treatment of the SIAM (with an additional self-consistency requirement) has been applied recently to obtain essentially exact results for the infinite- $d$  HM [16–19].

Nevertheless, it is necessary to develop and apply improved approximations to the  $d = \infty$  HM, because QMC yields its results along the imaginary time axis (or for the discrete Matsubara frequencies). Therefore, it is difficult to achieve results for very low temperatures, and an analytical continuation using the maximum entropy method is necessary to obtain the dependence of dynamical quantities on real frequency. Furthermore, because the mapping on the atomic or single-impurity problem is essential, the QMC treatments cannot be extended to finite  $d$ , for example, by means of a  $1/d$ -expansion. But the existing ‘essentially exact’ QMC results are very useful and important, as approximations may be applied to the same parameters (finite temperatures, etc) so that comparisons of the approximate results with the exact QMC results are possible now and allow for a judgment of the quality of the approximation.

When constructing improved approximations for the HM there exist several criteria that a meaningful approximation should fulfill. It should, of course, reproduce the trivial exactly solvable limits of vanishing correlation,  $U = 0$ , and the atomic limit (hopping  $t = 0$ ) should also be reproduced. Furthermore, for  $d = \infty$  the exact Brandt–Mielsch solution of the FKM should be reproduced, and for the general HM a (Mott–Hubbard) metal–insulator transition should exist for half-filling (occupation per spin direction  $n = 0.5$ ) and sufficiently strong interaction  $U$ . For a weak interaction  $U$ , however, the  $U$ -perturbation treatment and thus the Luttinger theorem and its consequences should be contained in a proper approach. Most of the existing approximations do not fulfill all of these criteria. Hubbard’s early treatments [1, 2] of the model are based on the equation of motion for the one-particle Green function. Naturally the free electron and atomic limit are fulfilled, and the lower and upper Hubbard band and a metal–insulator (Mott) transition are reproduced. Probably the description of this metal–insulator transition, as well as the description of the high-temperature properties, is already quite good within the Hubbard-III [2] (or the alloy

analogue) approximation; but these treatments violate the Luttinger theorem [10] at zero temperature,  $T = 0$ . The weak-coupling  $U$  perturbation theory is not reproduced, and the Fermi-liquid quasiparticles are absent, except for the trivial limit  $U = 0$ . There have been many attempts to improve Hubbard's treatment by means of higher-order equation of motion decouplings [20,21], but most of these treatments are also uncontrolled approximations and usually violate the Luttinger theorem [10] and do not exhibit Fermi-liquid behaviour. Another class of approximations is based on the weak-coupling perturbation theory with respect to the interaction strength  $U$ . The simplest non-trivial approximation within this scheme is the second-order  $U$ -perturbation treatment (SOPT), which can be studied either relative to the Hartree-Fock solution (SOPT-HF) [22,23] or fully self-consistently (SC-SOPT) [24]. The SOPT-HF has the advantage that at least in the symmetric case ( $n = 0.5$ ) the atomic limit is reproduced, whereas the SC-SOPT is the simplest conserving approximation in the Kadanoff-Baym scheme [11]. Such conserving approximations based on higher-order resummations of the  $U$ -perturbation series have been used recently by Bickers and co-workers [25] and by Serene and Hess [26]. The particle-hole  $T$ -matrix approximation for the self-energy, applied by one of us to the two-dimensional HM [27] also belongs to this class of conserving approximations; applications to the infinite-dimensional HM have been performed by Menge and Müller-Hartmann [28]. From these recent investigations [27,28] one also knows that these conserving approximations based on standard weak-coupling expansions and resummations properly fulfill the Luttinger theorem and the Fermi-liquid properties, but they fail to reproduce the metal-insulator transition [28]. This is certainly connected with the fact that these weak-coupling expansions usually do not properly reproduce the exactly solvable atomic limit.

From the above statements it is clear that it is highly desirable to use an approximation which contains both the weak-coupling limit (at least to some finite order in the interaction  $U$ ) to reproduce the Luttinger theorem and the Fermi-liquid properties, and the atomic limit to be able to reproduce a metal-insulator (Mott) transition for sufficiently large  $U$ . For the symmetric HM the SOPT-HF accidentally fulfils these requirements, i.e. it is exact up to order  $U^2$  and reproduces the atomic limit [23]. However, as indicated by the numerical results presented in this paper, Fermi-liquid behaviour never breaks down, i.e. the SOPT-HF does not contain a metal-insulator transition. An approximation, which away from half-filling also reproduces the atomic limit simultaneously with the second-order  $U$ -perturbation treatment, was suggested and investigated (for the single-impurity and periodic Anderson model) by Rodero and co-workers [29]. But in the symmetric case this approximation coincides with the SOPT-HF so that, again, the metal-insulator transition is missing in this approach. A different approximation fulfilling the requirements mentioned above was suggested by Edwards and Hertz [30]. They start from the Hubbard-III (alloy analogue) approximation, use an expansion of the corresponding approximate self-energy expression up to second order in  $U$ , and compare this expression with the correct finite-order SOPT result. By this means they construct an improvement of the alloy analogy simultaneously being correct up to order  $U^2$  in a weak-coupling expansion. First results presented in [30] show that this approach may yield very interesting and promising results, namely for half-filling a Fermi-liquid metallic regime, a non-Fermi-liquid regime and an insulating regime depending on the interaction strength  $U$ . But Edwards and Hertz did not present explicit results for the spectral function and self-energy obtained within their approximation. Furthermore, they used a model assumption for a certain spectral function characterizing the SOPT self-energy.

In the present paper we investigate the properties of this Edwards-Hertz approximation (EHA) [30] in some detail. We slightly reformulate this approximation and introduce, in particular, an effective atomic level  $E_{\sigma}$ , relative to which the  $U$ -perturbation treatment has

to be performed; in the symmetric case ( $n = 0.5$ )  $E_\sigma = E_0 + Un_{-\sigma}$  (where  $E_0$  is the bare atomic level position) corresponds to the Hartree level, for general filling  $n_\sigma E_\sigma$  has to be determined self-consistently. Looking only for paramagnetic solutions we apply this approach to the  $d = \infty$  HM (with a Gaussian unperturbed density of states) and calculate (without further additional model assumptions) the frequency dependence of the self-energy and spectral function for different correlation strengths  $U$ , fillings  $n$  and temperatures  $T$ . We confirm the existence of metallic Fermi-liquid and metallic non-Fermi-liquid phases and of a metal-insulator transition within this approach. For finite temperature we compare the results obtained within the EHA with 'essentially exact' QMC results [17] and find that qualitatively the overall features of the spectral function are fairly well reproduced. In particular, the metal-insulator transition occurs at a  $U$  of the correct magnitude. In detail, however, there are deviations between the EHA and the QMC results concerning, in particular, the magnitude of the (Mott-Hubbard) gap and the detailed reproduction of quasiparticle and separated satellite peaks. Therefore, in our opinion, it is still not clear how far the EHA prediction of a metallic non-Fermi-liquid phase is realistic.

The paper is organized as follows. Section 2 briefly describes the model, the basic definitions and our reformulation of the EHA. The numerical results obtained within this approach are presented and compared with QMC results in section 3. Section 4 contains a discussion of these results and our conclusion.

## 2. Model and Edwards-Hertz approximation

The Hubbard Hamiltonian is [1]

$$H = E_0 \sum_{R,\sigma} c_{R,\sigma}^\dagger c_{R,\sigma} + t \sum_{\langle R,R'\rangle,\sigma} c_{R,\sigma}^\dagger c_{R',\sigma} + U \sum_R c_{R,\uparrow}^\dagger c_{R,\uparrow} c_{R,\downarrow}^\dagger c_{R,\downarrow} \quad (1)$$

where  $\langle \rangle$  denotes the sum over nearest-neighbour vectors of a hypercubic lattice of dimension  $d$ ,  $\sigma$  is the spin index,  $E_0$  is the atomic energy,  $t$  the nearest-neighbour hopping matrix element and  $U$  is the on-site Coulomb interaction strength. The hopping term in the Hamiltonian is scaled so that the non-trivial limit is reached in the limit of infinite dimensions  $d \rightarrow \infty$ :  $4t^2d = t^{*2} = \text{constant}$ . For the assumed next-neighbour hopping on the  $d$ -dimensional hypercubic lattice we have

$$\epsilon_k = -\frac{t^*}{\sqrt{d}} \sum_{i=1}^d \cos k_i$$

with  $\mathbf{k} = (k_1, k_2, \dots, k_d)$ . The density of states (per spin direction) of the unperturbed (non-interacting) system has a Gaussian form [4]:

$$N^0(\omega) = \frac{1}{t^* \sqrt{\pi}} \exp[-(\omega/t^*)^2]. \quad (2)$$

A quantity of primary interest is the one-particle Green function  $G_\sigma(z)$  of the HM for arbitrary  $U$ :

$$G_\sigma(z) = \langle\langle c_{R,\sigma}; c_{R,\sigma}^\dagger \rangle\rangle = \int_{-\infty}^{\infty} d\omega \frac{N^0(\omega)}{z - \Sigma_\sigma(z) - \omega} = G^0(z - \Sigma_\sigma(z)) \quad (3)$$

which equation defines the self-energy  $\Sigma_\sigma(z)$  of the spin- $\sigma$  electrons,  $G^0(z)$  being the Green function of the uncorrelated system. The spectral function is obtained from the one-particle Green function according to

$$N_\sigma(\omega) = -\frac{1}{\pi} \text{Im} G_\sigma(\omega + i0). \quad (4)$$

We need a suitable approximation for the self-energy  $\Sigma_\sigma(z)$ . Following Edwards and Hertz [30] we use the following *ansatz*:

$$\Sigma_\sigma(z) = \frac{U n_{-\sigma}}{1 - (U - \Sigma_\sigma(z)) \tilde{G}_\sigma(z)} \quad (5)$$

where

$$n_\sigma = \int_{-\infty}^{\infty} d\omega' N_\sigma(\omega') f(\omega') \quad (6)$$

denotes the band filling (occupation number) of the spin- $\sigma$  electrons and  $f(\omega)$  the Fermi function:

$$f(\omega) = \left[ \exp\left(\frac{\omega - \mu}{k_B T}\right) + 1 \right]^{-1}.$$

Replacing  $\tilde{G}_\sigma(z)$  in (5) by the one-particle Green function  $G_\sigma(z)$  one obtains the usual CPA equation [31] corresponding to the alloy analogue (Hubbard-III) approximation for the HM. But following Edwards and Hertz we want to use an approximation for  $\tilde{G}_\sigma(z)$ , which reproduces the SOPT when expanding the self-energy expression (5) in powers of the Coulomb correlation  $U$  up to second order in  $U$ . This condition is fulfilled by the following approximation:

$$\tilde{G}_\sigma(z) = \int_{-\infty}^{\infty} d\omega' \frac{\tilde{N}_\sigma^0(\omega')}{z - \Sigma_\sigma(z) + E_\sigma - \omega'} \quad (7)$$

$$\begin{aligned} \tilde{N}_\sigma^0(\omega) = & \frac{1}{n_{-\sigma}(1 - n_{-\sigma})} \int_{-\infty}^{\infty} \int_{-\infty}^{\infty} \int_{-\infty}^{\infty} d\omega_1 d\omega_2 d\omega_3 N_{-\sigma}^0(\omega_1 - E_{-\sigma}) N_{-\sigma}^0(\omega_2 - E_{-\sigma}) \\ & \times N_{-\sigma}^0(\omega_3 - E_{-\sigma}) \{ f(\omega_1)[1 - f(\omega_2)] + f(\omega_3)[f(\omega_2) - f(\omega_1)] \} \delta(\omega + \omega_1 - \omega_2 - \omega_3). \end{aligned} \quad (8)$$

Here the shifts  $E_\sigma$  (leading to an effective atomic level for the  $\sigma$  electrons) have to be determined self-consistently so that the full occupation number  $n_\sigma$  appearing in (8) is equal to the unperturbed occupation corresponding to  $N_\sigma^0(\omega - E_\sigma)$ :

$$n_\sigma = \int_{-\infty}^{\infty} d\omega N_\sigma(\omega) f(\omega) = \int_{-\infty}^{\infty} d\omega N_\sigma^0(\omega - E_\sigma) f(\omega). \quad (9)$$

It is now easy to see that in the atomic limit (and also for the FKM), in which the unperturbed density of states (of the one  $-\sigma$  spin species for the FKM) is a delta function, one obtains:

$$\tilde{N}_\sigma^0(\omega) = N_\sigma^0(\omega - E_\sigma). \quad (10)$$

Therefore, according to (7) and (3) one gets in the atomic limit and for the FKM:

$$\tilde{G}_\sigma(z) = G_\sigma(z) = G^0(z - \Sigma_\sigma(z)) \quad (11)$$

and (5) reduces to the Hubbard-III (alloy analogue, CPA) condition. Therefore, the atomic limit and the exact Brandt-Mielsch solution [12] of the FKM are contained in the general approximation (5). Furthermore, a finite-order expansion of (5) up to second order in  $U$  yields

$$\Sigma_\sigma(z) = Un_{-\sigma} + U^2n_{-\sigma}(1 - n_{-\sigma})\tilde{G}_\sigma(z). \quad (12)$$

Here it is justified to use the zeroth-order (uncorrelated) occupation number  $n_{-\sigma}$  or the one corresponding to Hartree-Fock in the term already having a prefactor  $U^2$  and to replace the atomic level shift by zero or by the Hartree value  $Un_{\pm\sigma}$ , and one obviously recovers the standard SOPT expression of the perturbation theory up to second order in the correlation  $U$ , either in finite order or relative to Hartree-Fock. So the approximation (5) for the self-energy is exact up to second order in the correlation and it reproduces the atomic limit and the exact FKM solution for large  $d$ .

In their work Edwards and Hertz [30] did not introduce and discuss the effective atomic level shift  $E_\sigma$ , which is, however, essential to ensure that the EHA always (i.e. for arbitrary filling) reproduces the atomic limit and the exact solution of the FKM, because the prefactor  $[n_{-\sigma}(1 - n_{-\sigma})]^{-1}$  in (8) has to be cancelled. Only in the half-filled (symmetric) case is this shift relatively simple, namely  $E_\sigma = Un_{-\sigma} = U/2$ . Furthermore, [30] used the local approximation (of a  $k$ -independent, site-diagonal self-energy) as an additional *ad hoc* approximation, probably not knowing at that time that this becomes correct for  $d = \infty$ . Explicit numerical results for the frequency dependence of spectral function and self-energy were not presented in [30]. For the (relatively few) numerical results obtained so far, a semi-elliptic model density of states was used for  $N^0(\omega)$ , and an additional model assumption was used for  $\tilde{N}_\sigma^0(\omega)$ , which is essentially the spectral function corresponding to the SOPT self-energy. For our numerical calculations we use the Gaussian form for  $N^0$  (being appropriate for an infinite-dimensional hypercubic lattice) and we calculate the corresponding  $\tilde{N}_\sigma^0$  (i.e. avoid an additional *ad hoc* model assumption). The equations are solved iteratively, i.e. for given parameters  $U$  and temperature  $T$  and given occupation number  $n_\sigma$  we start from an initial guess for the chemical potential  $\mu$ , determine the atomic level shifts  $E_\sigma$  necessary for the given  $n_\sigma$  and calculate the modified spectral function  $\tilde{N}_\sigma^0(\omega)$ . As  $\tilde{G}(z)$  can be determined from  $\tilde{N}_\sigma^0(\omega)$  we can then solve the CPA-like equation (5) for the self-energy. The resulting full spectral function  $N_\sigma(\omega)$  allows for a new determination of  $\mu$  so that the pretended band filling is reproduced and the procedure is iterated until convergence is reached. Numerical results are presented in the following section.

### 3. Numerical results

For our numerical calculations we measure energies (frequencies) in units of the effective bandwidth  $t^* = 1$ , and look only for paramagnetic solutions; consequently, we can drop the spin indices in the equations. Figures 1–3 show the density of states  $N(\omega)$ , the imaginary part  $\text{Im}\Sigma(\omega + i0)$  and the real part of the self-energy  $\text{Re}\Sigma(\omega + i0)$  as a function of energy  $\omega$  for temperature  $T = 0$  K, an occupation (per spin direction)  $n = 0.5$  (symmetric half-filled HM) and a bare atomic level position  $E_0 = 0$ . In the half-filled system we have  $\mu = U/2 = E_{\pm\sigma}$ . Figure 1 shows the development of the density of states  $N(\omega)$  as a

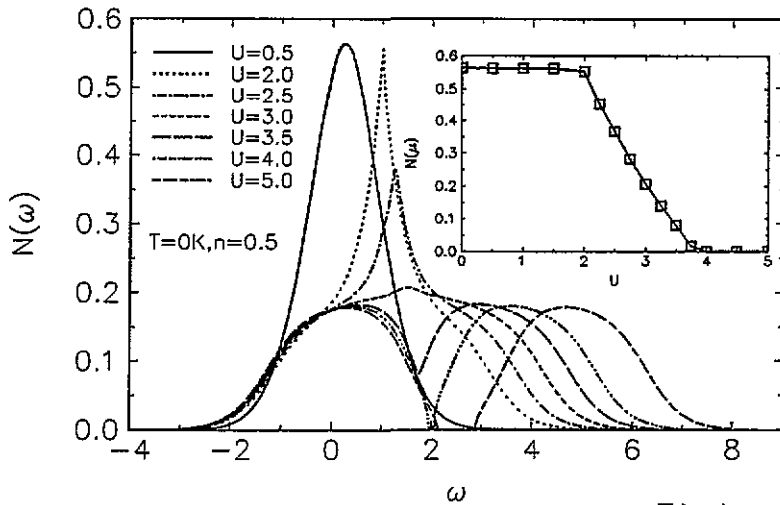


**Figure 1.** Density of states  $N(\omega)$  as a function of energy  $\omega$  for different interaction strengths  $U$ , band filling  $n = 0.5$  and temperature  $T = 0\text{K}$ . Inset: density of states  $N(\mu)$  at the chemical potential as a function of  $U$  for  $n = 0.5$ ,  $T = 0\text{K}$ .

function of frequency for different values of the interaction strength  $U$ . For very small  $U (= 0.5)$ ,  $N(\omega)$  has still essentially the Gaussian form characteristic of the uncorrelated system; up to  $U = 2$  there is still a peak at the chemical potential  $\mu = U/2$ , but the density of states also shows shoulders as precursors of the lower and upper Hubbard band. Increasing  $U$  further, the quasiparticle peak at  $\mu$  gradually becomes smaller and finally disappears, and for  $U \sim 4$  one obtains a splitting in an upper and lower Hubbard band and a Mott-Hubbard gap. Thus, as expected, the EHA contains both Fermi-liquid behaviour and a quasiparticle peak at the chemical potential in the weak-coupling regime and a metal-insulator transition for sufficiently strong interaction  $U > 4$ . The inset to figure 1 shows the value of the density of states at the Fermi level  $\mu$ . When the local approximation is valid,  $N(\mu)$  must be unrenormalized by the interaction (i.e. the same as for  $U = 0$ ) if the Fermi-liquid properties and the Luttinger theorem are fulfilled [8, 10]. This is valid up to  $U = 2$ , but for  $2 < U < 4$  there is a finite density of states at the Fermi level but with a smaller value than for  $U = 0$ ; this means that the system is conducting, but does not show Fermi-liquid behaviour, and for  $U > 4$  the system is a Mott insulator ( $N(\mu) = 0$ ). A curve very similar to that to the inset of figure 1 was obtained by Edwards and Hertz [30] for the semi-elliptic model density of states.

Figure 2 presents the imaginary part of the self-energy  $\text{Im}\Sigma(\omega + i0)$ . Close to  $U \approx 4$ , the imaginary part of the self-energy diverges at the chemical potential, in agreement with [30]. This behaviour is due to the fact that, for  $U < 4$ , equation (5) can be expanded around the chemical potential. For  $U > 4$  the series in  $U$  diverges and the solution of the modified CPA equation changes. The inset shows the imaginary part of the self-energy for small  $U$ . Obviously we see the quadratic vanishing near the chemical potential  $\mu$ ,  $\text{Im}\Sigma(\mu + \omega + i0) \sim \omega^2$ , which must be the case if the Luttinger theorem is fulfilled. But in the intermediate regime  $2 < U < 4$ ,  $\text{Im}\Sigma(\mu + i0)$  is finite, i.e. the Luttinger theorem is violated; for not too strong  $U$  there remain reminders of Fermi-liquid behaviour in form of a minimum in  $|\text{Im}\Sigma(\omega + i0)|$  at  $\mu$ . Beyond the value  $U = 4$ , the imaginary part of the self-energy develops a gap around the chemical potential  $\mu$ . Figure 3 demonstrates the energy dependence of the real-part of the self-energy  $\text{Re}\Sigma(\omega)$ . In particular, the behaviour of the real part for  $U = 3$  is interesting. The real part changes symmetry and the quasiparticle



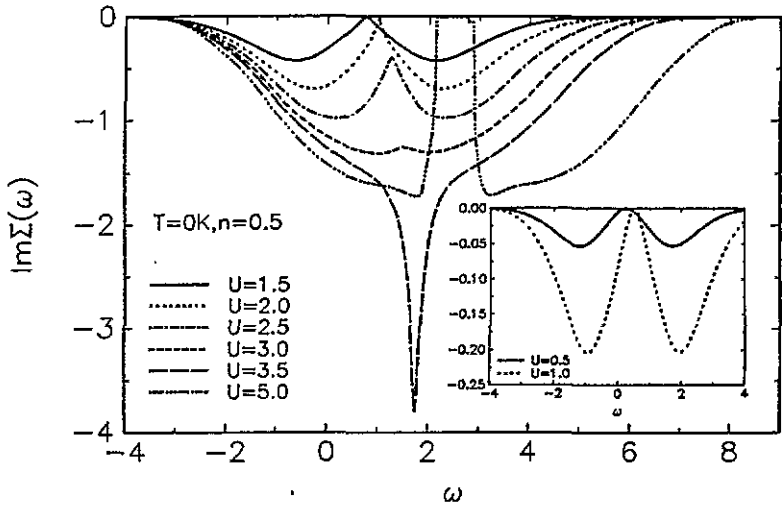


Figure 2. Imaginary part of the self-energy  $\Sigma(\omega)$  as a function of energy  $\omega$  for different interaction strengths  $U$ , band filling  $n = 0.5$  and temperature  $T = 0\text{ K}$ . Inset: imaginary part of the self-energy for  $U = 0.5, 1$  and  $T = 0\text{ K}$ ,  $n = 0.5$ .

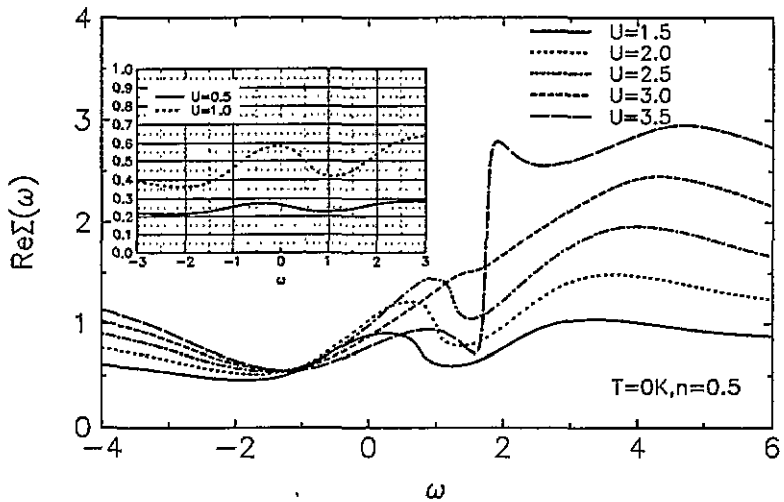


Figure 3. Real part of the self-energy  $\Sigma(\omega)$  as a function of energy  $\omega$  for different interaction strength  $U$ , band filling  $n = 0.5$  and temperature  $T = 0\text{ K}$ . Inset: real part of the self-energy for  $U = 0.5, 1$  and  $T = 0\text{ K}$ ,  $n = 0.5$ .

mass enhancement  $m^*/m = 1 - \partial\Sigma/\partial\omega|_{\omega=\mu}$  diverges for  $U \rightarrow 4$ . In the inset we present the real part of the self-energy for small interaction strength  $U$ , yielding the standard negative derivative at  $\mu$ , leading to a mass enhancement and being characteristic for a Fermi liquid.

In figure 4 we have plotted the density of states  $N(\omega)$  as a function of energy for  $U = 3$  for different band fillings  $n$  and  $T = 0\text{ K}$ . With decreasing  $n$  we again approach the Fermi-liquid regime, which is also present for larger values of  $U$  for small enough filling (occupation number). The value of the density of states at the chemical potential increases as we decrease the band filling  $n$ , and finally reaches the value of the uncorrelated density of states. In the inset we present the Gaussian density of states  $N^0(\omega)$  and the calculated effective spectral function  $\tilde{N}^0(\omega)$ , which vanishes quadratically with  $\omega$  at  $\mu - E_\sigma$ . If  $W$

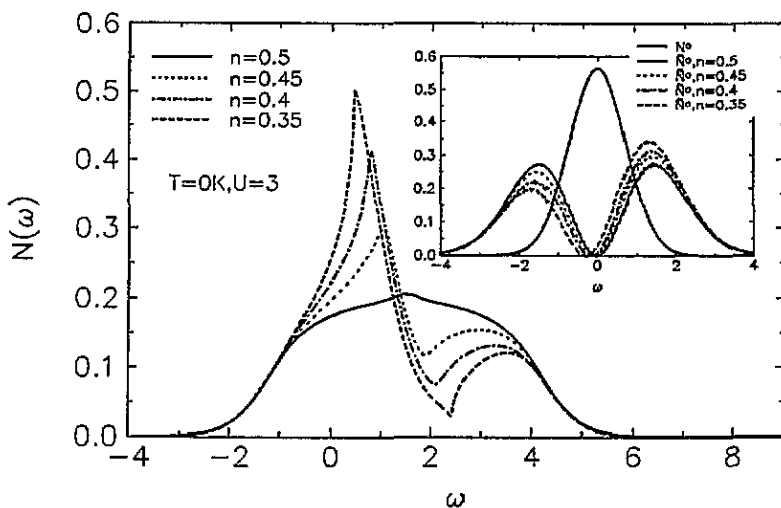


Figure 4. Density of states  $N(\omega)$  as a function of energy  $\omega$  for different band fillings  $n$  and for temperature  $T = 0\text{K}$ , interaction strength  $U = 3$ . Inset: density of states  $N^0(\omega)$  and  $\tilde{N}^0(\omega)$  as a function of energy for different band fillings  $n$  and  $T = 0\text{K}$ .

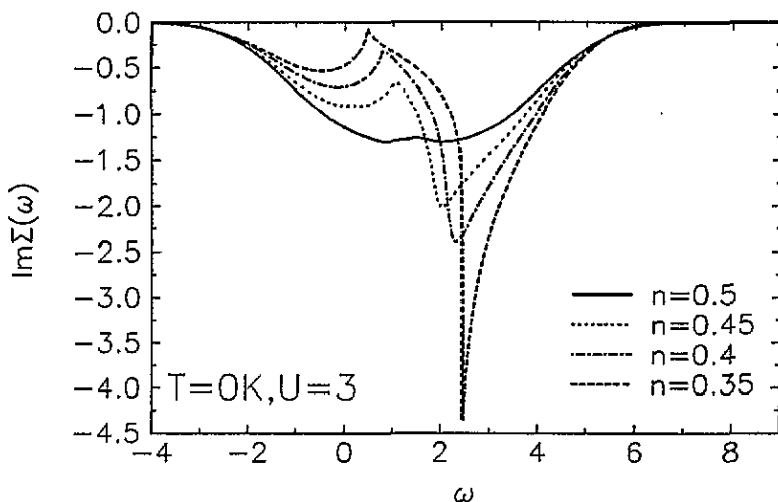


Figure 5. Imaginary part of the self-energy  $\Sigma(\omega)$  as a function of energy  $\omega$  for different band fillings  $n$  and for temperature  $T = 0\text{K}$ , interaction strength  $U = 3$ .

is a measure of the bandwidth of  $N^0(\omega)$  (truly the Gaussian density of states is non-zero for all energies) the bandwidth of  $\tilde{N}^0(\omega)$  is  $3W$ . The reason for this behaviour is a double convolution in the energy  $\omega$  in the expression for the density of states  $\tilde{N}^0(\omega)$ . The weight of  $\tilde{N}^0(\omega)$  below and above the Fermi energy is  $n$  and  $1 - n$  respectively. The tendency to approach again the Fermi-liquid regime with decreasing  $n$  is in agreement with results obtained in [30] and can also be seen from the self-energy imaginary part  $\text{Im}\Sigma(\omega + i0)$  shown in figure 5, in which a (quadratic) extremum develops with decreasing  $n$  which finally reaches  $\text{Im}\Sigma(\mu + i0) = 0$  in the Fermi-liquid phase.

In figures 6–9 we compare our numerical results for half-filling  $n = 0.5$  and for finite temperature  $\beta = 1/k_B T = 7.2$  with the SOPT-HF and with the QMC results of Pruschke and

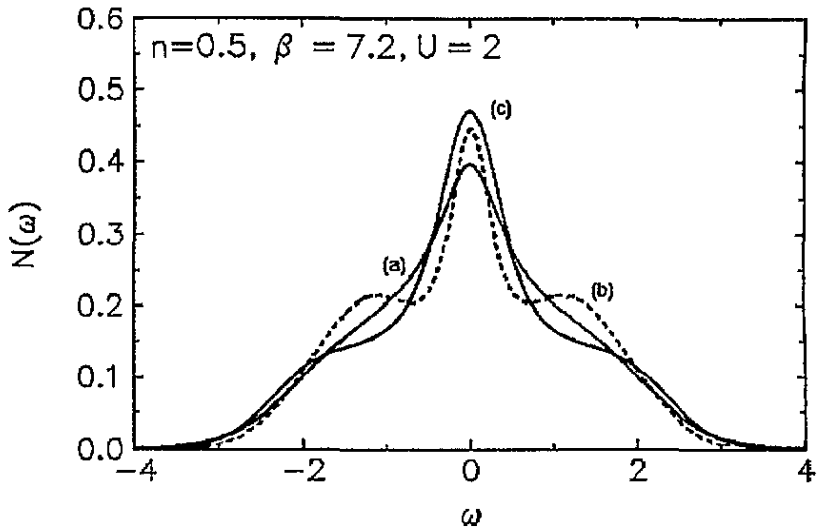


Figure 6. Density of states  $N(\omega)$  as a function of frequency  $\omega$  for band filling  $n = 0.5$ , interaction strength  $U = 2$ , and inverse temperature  $\beta = 1/k_B T = 7.2$ . (a) (EHA); (b): (QMC) [8]; (c): (SOPT).

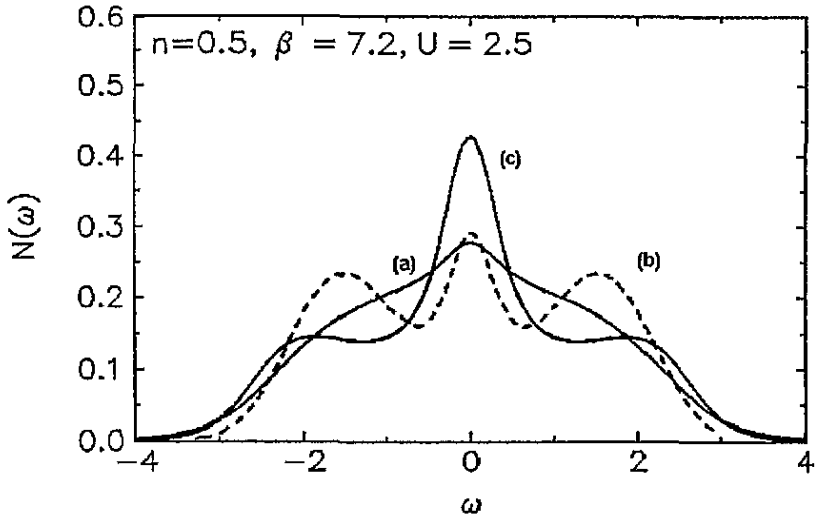


Figure 7. Density of states  $N(\omega)$  as a function of frequency  $\omega$  for band filling  $n = 0.5$ , interaction strength  $U = 2.5$ , and inverse temperature  $\beta = 1/k_B T = 7.2$ . (a) (EHA); (b): (QMC) [8]; (c): SOPT.

Jarrell [17] for different values of the interaction strength  $U$ ; here (and in the subsequent figures) the chemical potential  $\mu$  has been chosen as the zero point of the energy scale. The first observation is that the curves never coincide. For relatively small  $U$  the three curves are close together. With increasing  $U$ , SOPT and QMC results show satellite structures near  $E_0$  and  $E_0 + U$  as first indications of the lower and upper Hubbard band and, in addition, a quasiparticle peak around the chemical potential  $\mu = 0$ , whereas the EHA result shows only tiny shoulders near  $E_0$  and  $E_0 + U$  but no pronounced and well separated satellite bands. For  $U = 3$  (and even for larger values of  $U$ ) the SOPT-HF still yields the quasiparticle peak in addition to the upper and lower Hubbard band, but for both QMC and EHA results the quasiparticle peak has disappeared and only the upper and lower Hubbard band (not yet

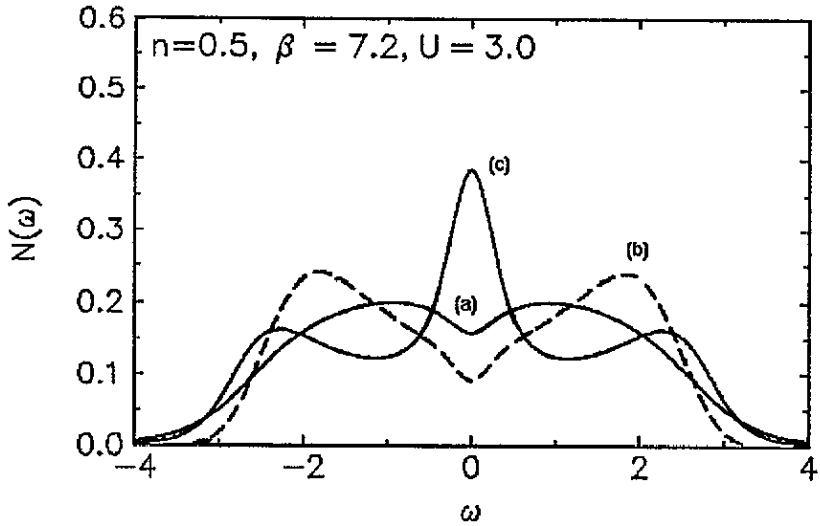


Figure 8. Density of states  $N(\omega)$  as a function of frequency  $\omega$  for band filling  $n = 0.5$ , interaction strength  $U = 3$ , and inverse temperature  $\beta = 1/k_B T = 7.2$ . (a) (EHA); (b): (QMC) [8]; (c): SOPF.

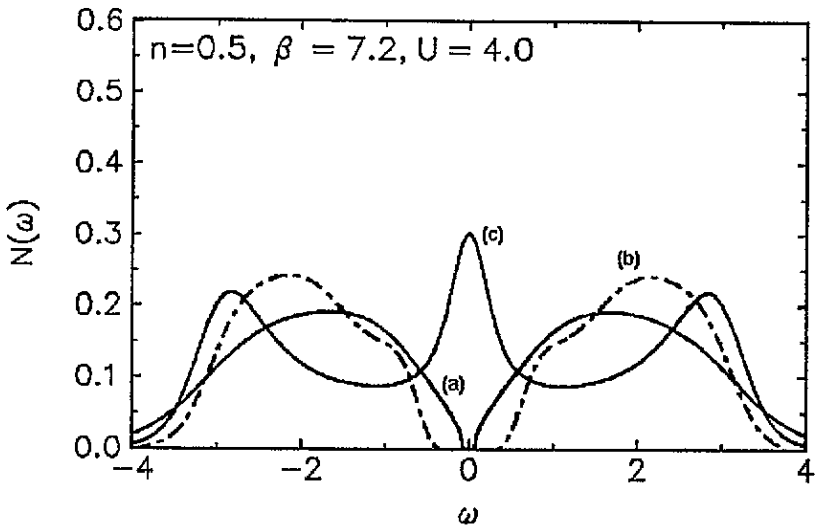


Figure 9. Density of states  $N(\omega)$  as a function of frequency  $\omega$  for band filling  $n = 0.5$ , interaction strength  $U = 4$ , and inverse temperature  $\beta = 1/k_B T = 7.2$ . (a) (EHA); (b): (QMC) [8]; (c): SOPF.

separated by a gap) are obtained. For  $U > 4$  both QMC and EHA yield a Mott-Hubbard insulator, the gap being, however, considerably smaller in the EHA compared to the QMC result. Therefore the qualitative tendency obtained and observed here in the EHA results agrees with the (essentially exact) QMC results. In particular, the EHA prediction of a metallic non-Fermi-liquid phase is not in contradiction with the available QMC results, as the absence of the quasiparticle peak for  $U = 3$  demonstrates. Of course, this quasiparticle peak can still develop for very low temperatures  $T$  inaccessible to QMC. Quantitatively and in detail, however, there are still deviations and discrepancies between QMC and EHA, in particular concerning the appearance of satellite (upper and lower Hubbard) bands separated from the quasiparticle peak in the weak-coupling regime and the width of the Mott-Hubbard gap in

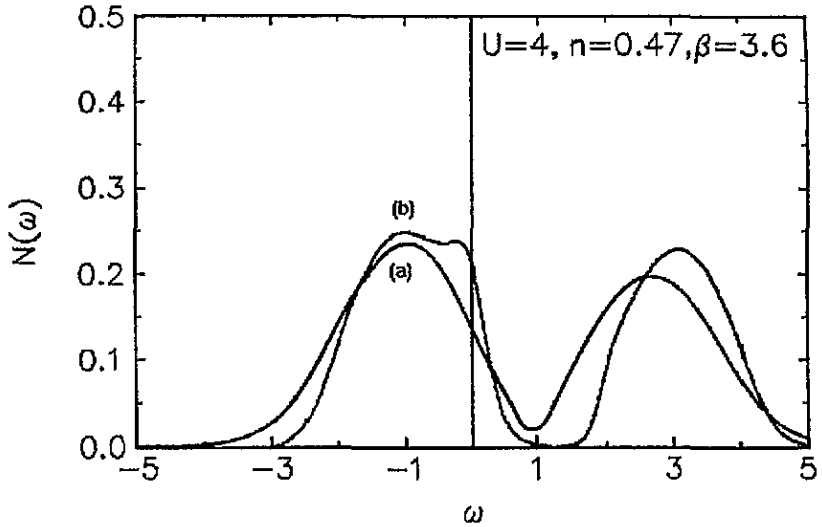


Figure 10. Density of states  $N(\omega)$  as a function of frequency  $\omega$  for band filling  $n = 0.47$ , interaction strength  $U = 4$ , and inverse temperature  $\beta = 1/k_B T = 3.6$ . (a) (EHA); (b): (QMC) [8].

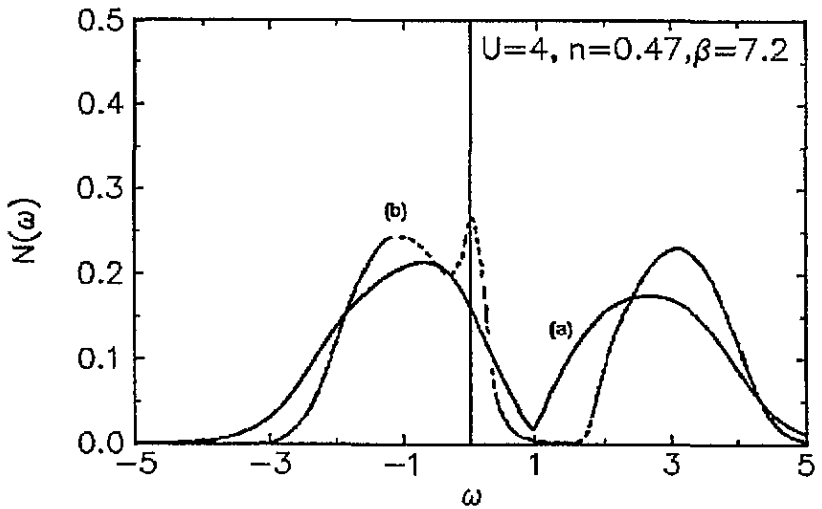
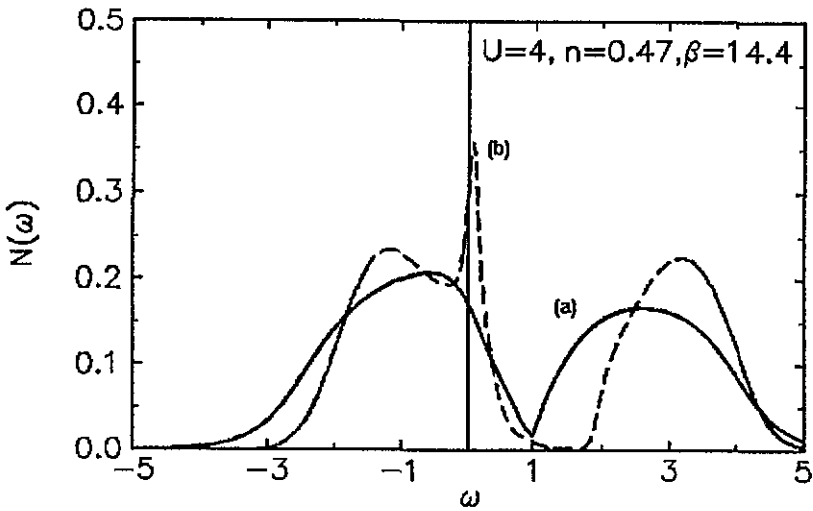


Figure 11. Density of states  $N(\omega)$  as a function of frequency  $\omega$  for band filling  $n = 0.47$ , interaction strength  $U = 4$ , and inverse temperature  $\beta = 1/k_B T = 7.2$ . (a) (EHA); (b): (QMC) [8].

the strong-coupling (insulating) regime.

Away from half-filling, comparisons between QMC and EHA are shown in figures 10–15. In figures 10–12 we show for  $n = 0.47$  and different temperatures  $T$  the EHA results and compare them with QMC results published by Pruschke and Jarrell [17]. For  $\beta = 1/k_B T = 3.6$  (figure 10) the curves are similar, though there are still deviations in detail. This changes for lower temperatures, see figure 12. In particular, the additional structure indicating the reappearance of a quasiparticle peak in the lower Hubbard band obtained in QMC is absent in the EHA. Again the (quasi) gap, which is situated away from the Fermi energy in the non-half-filled case, is too small in EHA compared to the QMC gap. In figures 13–15 the corresponding comparison between EHA and QMC is shown for fixed temperature  $\beta = 7.2$  and  $U = 4$  but different band filling. Obviously the agreement



**Figure 12.** Density of states  $N(\omega)$  as a function of frequency  $\omega$  for band filling  $n = 0.47$ , interaction strength  $U = 4$ , and inverse temperature  $\beta = 1/k_B T = 14.4$ . (a) (EHA); (b): (QMC) [8].

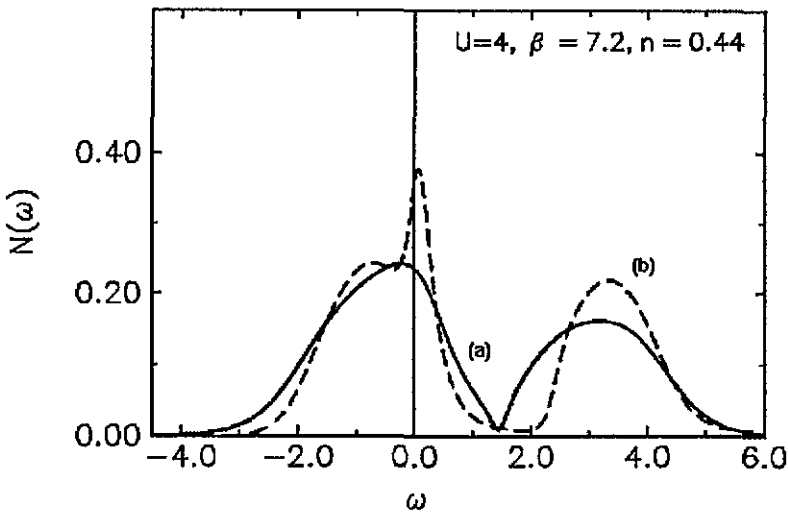


**Figure 13.** Density of states  $N(\omega)$  as a function of frequency  $\omega$  for band filling  $n = 0.44$ , interaction strength  $U = 4$ , and inverse temperature  $\beta = 1/k_B T = 7.2$ . (a) (EHA); (b): (QMC) [8].

between QMC and EHA improves with decreasing filling (see figure 15).

#### 4. Conclusion

In conclusion, we have presented a reformulation of the Edwards–Hertz approximation (EHA) [30], and we have applied the EHA to the Hubbard model in dimension  $d = \infty$  and presented the first detailed EHA calculations of spectral functions and self-energies. EHA is exact in the free-electron limit (vanishing correlation  $U$ ) and in the atomic limit (vanishing hopping  $t = 0$ ). Furthermore, in the weak-coupling limit the EHA agrees with the SOPT, i.e. when expanding the EHA expression for the self-energy in a series in powers

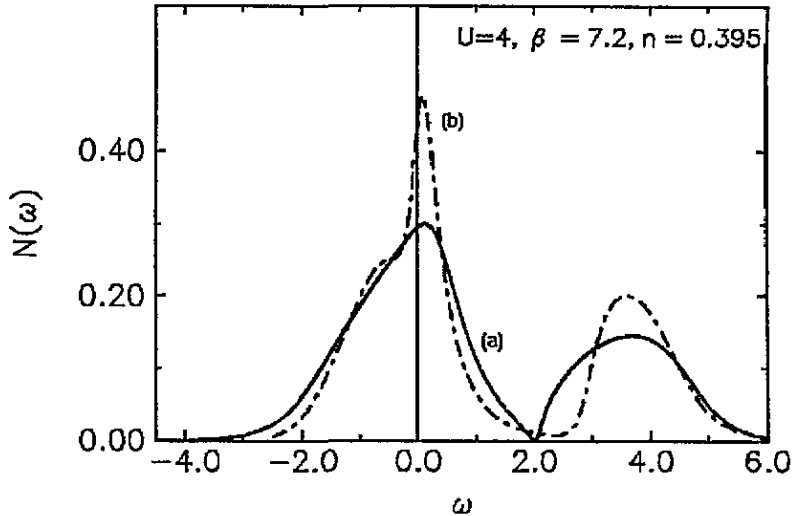


Figure 14. Density of states  $N(\omega)$  as a function of frequency  $\omega$  for band filling  $n = 0.395$ , interaction strength  $U = 4$ , and inverse temperature  $\beta = 1/k_B T = 7.2$ . (a) (EHA); (b): (QMC) [8].

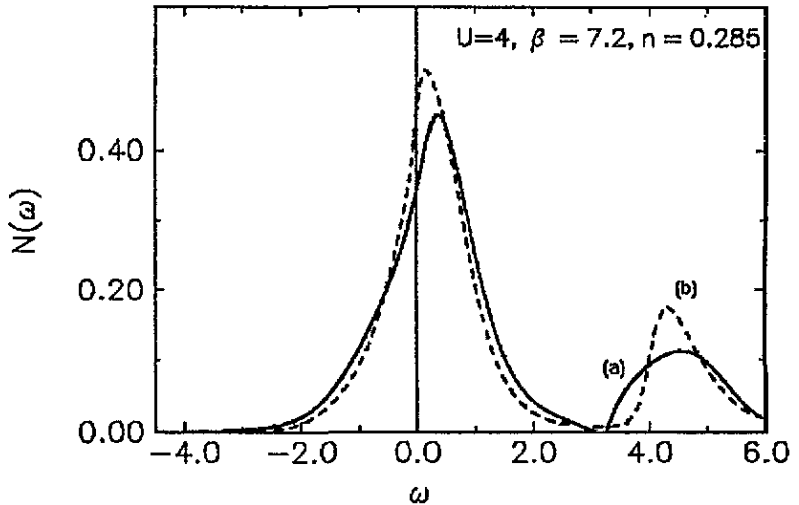


Figure 15. Density of states  $N(\omega)$  as a function of frequency  $\omega$  for band filling  $n = 0.285$ , interaction strength  $U = 4$ , and inverse temperature  $\beta = 1/k_B T = 7.2$ . (a) (EHA); (b): (QMC) [8].

of the correlation strength  $U$  one obtains agreement with the standard (Feynman diagram) expansion up to order  $U^2$ . Even in higher orders in  $U$  (where the EHA is no longer exact) the conditions of the Luttinger theorem are fulfilled. Furthermore, when applied to the Falicov–Kimball model (FKM) (i.e. if the electrons of the  $-\sigma$  spin direction are frozen and cannot hop) the EHA expression for the self-energy (of the spin  $+\sigma$  electrons) reduces to the alloy analogue approximation (CPA). Thus the exact (Brandt–Mielsch [12]) solution of the  $d = \infty$  FKM is also reproduced within the EHA. Judged from the reproduction of exactly known limits the EHA appears to be one of the best existing general approximation schemes for the HM (at least for  $d = \infty$ ). It can be considered as a generalization of the Hubbard–III approximation so that the weak-coupling limit up to order  $U^2$  is reproduced, and it can also be considered as a generalization of the SOPT so that the atomic limit is fulfilled

and an application to the strong-coupling regime (to an investigation of the Mott-Hubbard metal-insulator transition) is possible.

The results for the spectral function and self-energy show a clear indication of Fermi-liquid behaviour for small interaction ( $U < 2$ ), as the self-energy imaginary part vanishes quadratically at the chemical potential  $\mu$  and as a quasiparticle peak exists and the density of states at the Fermi level is unaffected by the interaction. For strong interaction ( $U > 4$ ) and half-filling the EHA predicts a Mott insulator. Thus the EHA is able to describe a metal-insulator transition and a crossover from a weak-coupling Fermi-liquid phase to a strong-coupling insulating phase. For intermediate-coupling strength ( $2 < U < 4$ ), however, the EHA yields a metallic non-Fermi-liquid phase indicated by the fact that the absolute value of the self-energy imaginary part has only a minimum but does not vanish at  $\mu$ , and by a reduction of the density of states value at  $\mu$  compared to the uncorrelated ( $U = 0$ ) value. To judge the reliability of these results we compared them with available 'essentially exact' results obtained by Pruschke and Jarrell [17] using a mapping on the SIAM (with the hybridization and effective conduction band to be determined self-consistently) and a QMC treatment of this effective SIAM. On an overall scale we find qualitatively reasonable agreement between the QMC and the EHA results. In detail and quantitatively, however, there are also deviations and discrepancies, in particular concerning the reproduction of the upper and lower Hubbard band and simultaneously a quasiparticle band, and also concerning the width of the Mott-Hubbard gap. Therefore, particularly for intermediate values of the correlation, the reliability of the EHA results is not yet clear, though also the existing QMC results do not exclude the possibility of a metallic non-Fermi-liquid phase. We did not analyse in detail the nature of the metallic non-Fermi-liquid state found here, because we believe that it should first be clarified if this state is an artefact of the EHA or if it is realistic (this could be done by investigating, for instance, if such a state persists in improved versions of the EHA).

In the future the EHA can, of course, be applied to the investigation of other interesting properties; for the  $d = \infty$  Hubbard model one can calculate correlation functions (susceptibilities and transport quantities) and one should look for the existence of antiferromagnetic and ferromagnetic solutions. In our opinion, only after this investigation for magnetic solutions is completed (an investigation that is currently under way), will the construction of a phase diagram in the  $U$ - $n$  plane (probably containing a paramagnetic metallic Fermi-liquid, a non-Fermi-liquid, an insulating phase and magnetic phases) be meaningful. Furthermore, applications of this approximation (or slightly reformulated versions of it) to other models like the SIAM, the PAM or the localized ( $f$ -) self-energy of the FKM should be possible. On the other hand, improvements of the EHA are certainly necessary and should be possible. As mentioned in the introduction, it must be possible to express the self-energy as a functional of the local Green function,  $\Sigma(z) = S[G(z)]$ . The EHA formulation does not provide for (an approximation of) the functional dependence on  $G(z)$ . An approximation for the functional  $S[G]$  being at least as good as the EHA could be directly applied to the other models mentioned above. Very recently, Li and d'Ambrumenil [32] tried to formulate an approximate functional for the  $d = \infty$  HM, but in their approximation they do not find a Mott transition at a finite value of  $U$  so that their approximation seems to be worse than the EHA discussed here. In a recent paper Edwards [33] pointed out by means of a diagrammatic analysis that in the local approximation (i.e. for  $d = \infty$ ) it should be possible to express the self-energy as a functional of  $G/(1 + \Sigma G)$ :  $\Sigma(z) = S_1[G/(1 + \Sigma G)]$ . We would like to stress, however, that the EHA does not give an approximation for the functional  $S_1$ , either. In the EHA the self-energy is given as a functional  $S[\tilde{G}]$  or  $S_1[\tilde{G}/(1 + \Sigma\tilde{G})]$ , where  $\tilde{G}$  is the effective Green function essentially corresponding to the SOPT self-energy,



but *not* as a functional of the local one-particle Green function  $G$  as it should be according to the diagram analysis for  $d = \infty$ . A modified approximation, which has all the advantages of the EHA but uses an explicit functional  $S[G]$  or  $S_1[G/(1 + \Sigma G)]$  for the self-energy, is currently under investigation by us. Of course one can also try to develop improvements of the EHA, which reproduce the  $U$  perturbation beyond the second order in  $U$  or which simultaneously reproduce the perturbation series around the atomic limit.

### Acknowledgment

This work has been supported by the Deutsche Forschungsgemeinschaft (project Cz 31/5-2).

### References

- [1] Hubbard J 1963 *Proc. R. Soc. A* **276** 238
- [2] Hubbard J 1964 *Proc. R. Soc. A* **281** 401
- [3] Lieb E H and Wu F Y 1968 *Phys. Rev. Lett.* **20** 1445
- [4] Metzner W and Vollhardt D 1989 *Phys. Rev. Lett.* **62** 324
- [5] Vollhardt D 1993 *Correlated Electron Systems* ed V J Emery (Singapore: World Scientific) p 57
- [6] Janis V 1991 *Z. Phys. B* **83** 227; 1989 *Phys. Rev. B* **40** 11331
- [7] Janis V and Vollhardt D 1992 *Int. J. Mod. Phys. B* **6** 731
- [8] Müller-Hartmann E 1989 *Z. Phys.* **76** 211
- [9] Schweitzer H and Czycholl G 1989 *Solid State Commun.* **69** 171
- [10] Luttinger J M 1960 *Phys. Rev.* **119** 1153
- [11] Baym G and Kadanoff L P 1961 *Phys. Rev.* **124** 287  
Baym G 1962 *Phys. Rev.* **127** 1391
- [12] Brandt U and Mielsch C 1989 *Z. Phys. B* **75** 365; 1990 *Z. Phys. B* **79** 295; 1991 *Z. Phys. B* **82** 37
- [13] Georges A and Kotliar G 1992 *Phys. Rev. B* **45** 6479
- [14] Faficov L M and Kimball J C 1969 *Phys. Rev. Lett.* **22** 997
- [15] Gieseke A and Brandt U 1993 *Phys. Rev. B* **48** 10311
- [16] Jarrell M 1992 *Phys. Rev. Lett.* **69** 168
- [17] Jarrell M and Pruschke Th 1993 *Z. Phys. B* **90** 187
- [18] Rozenberg M J, Zhang X Y and Kotliar G 1992 *Phys. Rev. Lett.* **69** 1236  
Georges A and Krauth W 1992 *Phys. Rev. Lett.* **69** 1240
- [19] Zhang X Y, Rozenberg M J and Kotliar G 1993 *Phys. Rev. Lett.* **70** 1666
- [20] Cyrot M 1977 *Physica B* **91** 141
- [21] Czycholl G 1985 *Phys. Rev. B* **31** 2867
- [22] Bulk G and Jelitto R J 1990 *Phys. Rev. B* **41** 413
- [23] Schweitzer H and Czycholl G 1991 *Z. Phys. B* **83** 93
- [24] Müller-Hartmann E 1989 *Z. Phys. B* **74** 507
- [25] Bickers N E, Scalapino D J and White S R 1989 *Phys. Rev. Lett.* **62** 961  
Bickers N E and White S R 1991 *Phys. Rev. B* **43** 8044
- [26] Serene J W and Hess D W 1991 *Phys. Rev. B* **44** 3391
- [27] Werbter S and Tewordt L 1993 *Physica C* **211** 132; 1993 *Phys. Rev. B* **48** 10514
- [28] Menge B and Müller-Hartmann E 1991 *Z. Phys. B* **82** 237
- [29] Martin-Rodero A, Louis E, Flores F and Tejedor C 1986 *Phys. Rev. B* **33** 1814
- [30] Edwards D M and Hertz J A 1990 *Physica B* **163** 527
- [31] Elliot R J, Krumhansl J A and Leath P L 1974 *Rev. Mod. Phys.* **46** 465
- [32] Li Y M and d'Ambrumenil N 1993 *Preprint*
- [33] Edwards D M 1993 *J. Phys.: Condens. Matter* **5** 161